Altitude effect on leaf wax carbon isotopic composition in humid tropical forests

Mong Sin Wu [a], Sarah J. Feakins [a,*], Roberta E. Martin [b], Alexander Shenkin [c], Lisa Patrick Bentley [c,1], Benjamin Blonder [c], Norma Salinas [c,2], Gregory P. Asner [b], Yadvinder Malhi [c]

[a] Department of Earth Sciences, University of Southern California, 3651 Trousdale Pkwy, Los Angeles, CA 90089, USA
[b] Department of Global Ecology, Carnegie Institution for Science, 260 Panama St, CA 94305, Stanford, USA
[c] Environmental Change Institute, School of Geography and the Environment, University of Oxford, South Parks Road, Oxford OX1 3QY, UK

Abstract

The carbon isotopic composition of plant leaf wax biomarkers is commonly used to reconstruct paleoenvironmental conditions. Adding to the limited calibration information available for modern tropical forests, we analyzed plant leaf and leaf wax carbon isotopic compositions in forest canopy trees across a highly biodiverse, 3.3 km elevation gradient on the eastern flank of the Andes Mountains. We sampled the dominant tree species and assessed their relative abundance in each tree community. In total, 405 sunlit canopy leaves were sampled across 129 species and nine forest plots along the elevation profile for bulk leaf and leaf wax n-alkane (C_{27}–C_{33}) concentration and carbon isotopic analyses ($\delta^{13}C$); a subset (76 individuals, 29 species, five forest plots) were additionally analyzed for n-alkanoic acid (C_{22}–C_{32}) concentrations and $\delta^{13}C$. $\delta^{13}C$ values display trends of $+0.87 \pm 0.16\%o$ km^{-1} (95% CI, $r^2 = 0.96$, $p < 0.01$) for bulk leaves and $+1.45 \pm 0.33\%o$ km^{-1} (95% CI, $r^2 = 0.94$, $p < 0.01$) for C_{29} n-alkane, the dominant chain length. These carbon isotopic gradients are defined in multi-species sample sets and corroborated in a widespread genus and several families, suggesting the biochemical response to environment is robust to taxonomic turnover. We calculate fractionations and compare to adiabatic gradients, environmental variables, leaf wax n-alkane concentrations, and sun/shade position to assess factors influencing foliar chemical response. For the 4 km forested elevation range of the Andes, 4–6‰ higher $\delta^{13}C$ values are expected for upland versus lowland C_3 plant bulk leaves and their n-alkyl lipids, and we expect this pattern to be a systematic feature of very wet tropical montane environments. This elevation dependency of $\delta^{13}C$ values should inform interpretations of sedimentary archives, as ^{13}C-enriched values may derive from C_4 grasses, petrogenic inputs or upland C_3 plants. Finally, we outline the potential for leaf wax carbon isotopes to trace biomarker sourcing within catchments and for paleoaltimetry.
© 2017 Elsevier Ltd. All rights reserved.

1. INTRODUCTION

* Corresponding author.
   E-mail address: feakins@usc.edu (S.J. Feakins).
[1] Department of Biology, Sonoma State University, 1801 East Cotati Avenue, Rohnert Park, CA 94928, USA.
[2] Permanent address: Seccion Química, Pontificia Universidad Católica del Perú, Peru.

Plant leaf wax biomarkers and their carbon isotopic composition ($\delta^{13}C_{wax}$) have found application for sedimentary sourcing (Galy et al., 2011; Tao et al., 2015; Häggi et al., 2016; Hemingway et al., 2016) and paleoenvironmental reconstruction (Freeman and Colarusso, 2001; Huang

et al., 2001; Schefuß et al., 2003; Feakins et al., 2005; Whiteside et al., 2010; Tipple et al., 2011). Modern plant sampling have built a foundation for biomarker-based reconstructions (Collister et al., 1994; Chikaraishi and Naraoka, 2003; Bi et al., 2005; Garcin et al., 2014). With relevance to tropical C_3 forests the data are limited, however a survey in west-central Africa has found a trend toward higher $\delta^{13}C_{wax}$ in C_3 plants with increasing aridity (Vogts et al., 2009; Garcin et al., 2014; Badewien et al., 2015). Within canopies there are also vertical gradients (up tree) in $\delta^{13}C_{wax}$ (Graham et al., 2014). Although our theoretical understanding of plant carbon fixation and fractionation is high, we have gaps in knowledge of plant wax traits at the ecosystem-scale (Diefendorf and Freimuth, 2017). In particular, we need broad sampling of productive, canopy foliage in highly biodiverse, tropical forests (Freeman and Pancost, 2014), toward source-to-sink carbon cycle studies in tropical montane catchments and paleoenvironmental reconstructions.

1.1. ^{13}C fractionation during carbon fixation and growth of plant leaves

The carbon isotopic composition of plant organic matter is a product of atmospheric conditions and plant biogeochemistry associated with the fixation of atmospheric CO_2 (Farquhar et al., 1989). Extensive research has catalogued the environmental sensitivity of carbon isotopic fractionations in C_3 plants in natural ecosystems and experimental settings (see Cernusak et al., 2013 for a recent review). Most theory developed from measurements on bulk leaf ($\delta^{13}C_{leaf}$). $\delta^{13}C_{leaf}$ represents the average of all biochemicals within the leaf at time of measurement, each the product of many biosynthesis steps. Variable proportions of non-structural carbohydrates such as starches and simple sugars are exported from the leaf (Hoch and Körner, 2012) and proportions of the foliar constituents (lignin, cellulose etc.) vary between species and across environmental gradients (Asner et al., 2014b, 2016). Nevertheless, $\delta^{13}C_{leaf}$ represents a convenient metric for the assessment of the relative fractionation of specific compounds.

1.2. ^{13}C fractionation during plant wax biosynthesis in C_3 plants

Compound-specific approaches isolate a class of biomarkers for carbon isotopic analysis, for example the *n*-alkanes, *n*-alkanoic acids or *n*-alcohols, commonly present in the cuticular and epicuticular waxes on a plant leaf (Eglinton and Hamilton, 1967), and of these the *n*-alkanes are the most commonly applied to paleoenvironmental reconstructions. Although compound-specific approaches routinely collect data on multiple homologues within a series (Garcin et al., 2014), often one chain length will be selected for sedimentary reconstructions, perhaps most often the C_{29} *n*-alkane ($\delta^{13}C_{29alk}$). Compound-specific isotopic compositions reflect the net fractionation from a sequence of biosynthesis steps; the pathway for production of *n*-alkyl lipids are known (Zhou et al., 2010) and the isotopic composition of different chain lengths and compound

classes have been reported (Chikaraishi and Naraoka, 2007). However, theory and applications would benefit from a more comprehensive assessment of biomarker isotopic compositions in natural ecosystems and experimental settings (Freeman and Pancost, 2014). Paired measurements of compound-specific and bulk carbon isotopic compositions would help to capitalize on decades of $\delta^{13}C_{leaf}$ research and established theory for C-fixation to build understanding of post-photosynthetic fractionation processes (Brüggemann et al., 2011).

1.3. Altitude effect on $\delta^{13}C$ in humid ecosystems

Altitudinal transects have revealed that $\delta^{13}C_{leaf}$ values increase with elevation by *c.* 1‰ km^{-1} in non-water-stressed regions (Körner et al., 1988, 1991), but the relationship may break down in arid regions (Friend et al., 1989). Globally, $\delta^{13}C_{leaf}$ values in C_3 plants show mean annual precipitation (MAP) as the primary variable, with elevation the secondary variable (Diefendorf et al., 2010). But, the precipitation relationship is logarithmic, with greater sensitivity at lower MAP (when plants restrict stomatal exchange of water and indirectly CO_2), and very little sensitivity in very wet climates (when stomata are open). Between 250 mm (semi-arid) and 1.5 m MAP $\delta^{13}C$ values decrease by *c.* 6‰, but <1‰ further decrease occurs between 1.5 and 3.75 m MAP (Diefendorf et al., 2010). Elevation is therefore expected to dominate in wet climates.

Humid tropical forests drape the eastern flank of the Andes, and yield a $\delta^{13}C_{leaf}$ increase with elevation (Asner et al., 2014b). In this ecological survey and elevation-$\delta^{13}C$ biomarker calibration effort, we resample that profile and extend analyses to individual leaf wax compounds, to survey post-photosynthetic carbon isotope biogeochemistry. We greatly expand the available data on leaf wax carbon isotopic compositions and fractionations, and provide landscape-level information with which to characterize tropical forests from lowland and montane regions. This follows prior reports of elevation responses in the leaf wax δD values (Feakins et al., 2016a) and in the concentration and productivity of *n*-alkanes with elevation (Feakins et al., 2016b) in the same forest plots; as well as δD gradients in river-exported leaf wax in the same watershed (Ponton et al., 2014). Establishing the gradient of plant biomarker $\delta^{13}C$ with elevation in this transect contributes to the study of source-to-sink carbon cycling and paleoenvironmental reconstructions. The degree to which the findings can be generalized to other elevation profiles (and to paleoaltimetry) will depend on geographic (and temporal) differences in climate and ecosystem type (Körner, 2007).

2. MATERIALS AND METHODS

2.1. Study sites

This study includes nine plots (Fig. 1; Table 1) that belong to a group of permanent 1-ha plots operated by the Andes Biodiversity Ecosystems Research Group (ABERG, http://www.andesconservation.org) and that are part of the ForestPlots (https://www.forestplots.net/)
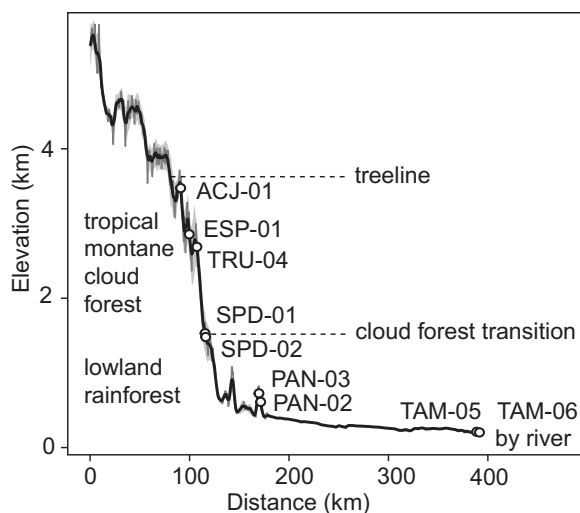
Fig. 1. Location of nine forest plots on an elevation transect along the eastern flank of Andes in southern Perú. Site locations (open circles, site name annotated, vegetation zones, cloud base, and river proximity are indicated. Elevation profile: grey line (elevation acquired from the Shuttle Radar Topographic Mission (SRTM) 90 m Digital Elevation Database 4.1 (Reuter et al., 2007), black line (smoothed elevation), grey envelope ($\pm 2\sigma$ elevation from 1 km-wide swath perpendicular to transect, re-centered to smoothed elevation). For an interactive map of study locations see Appendix A.

and Global Ecosystems Monitoring Network (GEM; http://gem.tropicalforests.ox.ac.uk/projects/aberg). Five montane plots (ACJ-01, ESP-01, TRU-04, SPD-01, SPD-02) are located in the Kosñipata Valley in the province of Paucartambo, in the department of Cusco, Perú; two

submontane plots (PAN-03, PAN-02) are located in the Pantiacolla front range of the Andes, and two lowland plots (TAM-05, TAM-06) are located in Tambopata, in the department of Madre de Dios, Perú (Fig. 1, Table 1). All plots have relatively homogeneous soil substrates and stand structure, and minimal evidence of human disturbance (Girardin et al., 2014). The lowland plots were established in the early 1980 s, and the montane ones between 2003 and 2013, with all stems $\geq$10 cm diameter at breast height tagged and identified to species-level, and plots have been annually measured for carbon allocation and cycling following the standard GEM Network protocol (Marthews et al., 2014). The productivity and carbon dynamics of these plots have been reported in Malhi et al. (2016).

2.2. Climate

Climate is humid throughout the elevation gradient, with mean annual precipitation (MAP) ranging from 1.5 to 5.3 m yr^{-1}, with peak precipitation at *c.* 1.5 km elevation in the lower montane cloud forests (Table 1). Mean annual temperature decreases with increasing elevation from 24.4 °C to 9 °C. Relative humidity is consistently high, typically >90%, but ranges from 75.2 to 93.7%, and estimated Vapor Pressure Deficit (VPD) for plants ranges from 0.05 to 0.75 kPa (Goldsmith et al., 2016). Along the transect from 0.2 to 3.5 km elevation, the atmospheric pressure and hence the partial pressure of CO_2 (pCO_2) decreases adiabatically following the equation:

$$\text{Equivalent } pCO_2 = P_0 \times e^{-h/h_0} \qquad (1)$$

where P_0 is the pCO_2 at sea level, h is the elevation, and h_0 (approximately 8.5 km at 290 K) is the scale height of

Table 1
Environmental and ecological characteristics of 1-ha study plots along a tropical montane elevation gradient, together with sample size and representation.

CHAMBASA Site	TAM-06	TAM-05	PAN-02	PAN-03	SPD-02	SPD-01	TRU-04	ESP-01	ACJ-01
Latitude	−12.839	−12.831	−12.650	−12.638	−13.049	−13.048	−13.106	−13.175	−13.147
Longitude	−69.296	−69.271	−71.263	−71.274	−71.537	−71.542	−71.589	−71.595	−71.632
Elevation[*] (m)	215	223	595	859	1494	1713	2719	2868	3537
Slope[*] (deg)	2.2	4.5	11.5	13.7	27.1	30.5	21.2	27.3	36.3
Aspect[*] (deg)	169	186	138	160.5	125	117	118	302	104
Mean annual air temp.[**] (°C)	24.4	24.4	23.5[**]	21.9[**]	18.8	17.4	13.5	13.1	9
Precipitation (mm yr^{-1})	1900	1900	2366[**]	2835[**]	5302	5302	2318	1560	1980
Relative humidity (%)[a]	84.5	84.5	75.2	75.2	93.7	93.7	86.2	89.1	93.3
Vegetation height[*]	28.2	27.5	24.4	18.7	22.8	14	15.7	16.9	12.5
pCO_2 equivalency (ppm)[b]	389	389	372	361	335	327	291	286	265
Sampled plant families	11	15	9	10	17	20	10	10	8
Sampled plant genera	14	21	10	14	21	22	11	10	8
Sampled plant species	15	24	11	15	22	26	14	13	11
Sampled plant individuals	38	58	25	36	57	58	49	44	40
Basal area represented (%)[c]	18.3	45.9	29.0	33.2	53.4	36.5	43.6	63.4	72.9

[*] Derived from high-resolution airborne Light Detection and Ranging (LiDAR) data (see Asner et al., 2014a for methodology).
[**] Derived from observations between 6 February 2013 and 7 January 2014.
[a] Goldsmith et al. (2016).
[b] Estimated based on elevation. See details in Section 2.2 for methodology.
[c] For *n*-alkanes and bulk samples. Basal area represented by sampled species as a proportion of all trees for the *n*-alkane survey. Data for *n*-alkanoic acids are taken from a subset, with lower basal area representation.

Earth's atmosphere. We have taken a sea level pCO_2 at 394 ppmv as of 1-yr average prior to sampling in measured at Mauna Loa (Scripps CO_2 Program; Keeling et al., 2001). We add 5 ppmv to reflect the higher CO_2 concentrations in the Amazon canopy compared to the free atmosphere (Olsen and Randerson, 2004), although diurnal cycles are about 100 ppmv, these are assumed constant across the profile. Thus, sampling across the 0.2–3.5 km elevation transect is equivalent to sampling from 389 to 265 ppmv pCO_2. For the same year the mean atmospheric $\delta^{13}C_{CO_2}$ reported from Mauna Loa is −8.4‰ (Keeling et al., 2001).

2.3. Collection of canopy leaf samples

Canopy leaf samples were collected as part of the CHAMBASA (CHallenging Attempt to Measure Biotic Attributes along the Slopes of the Andes) project from April – November 2013. Trees were chosen based on the most recently available census of tree diameter data. A sampling protocol was adopted wherein species were sampled that maximally contributed to plot basal area (a proxy for plot biomass or crown area). Within each species, three to five largest individual trees were chosen for sampling (five trees in upland sites and three trees in lowland sites depending on species diversity and practical time constraints). When a certain individual was not available (due to death, tree fall, or inaccessibility), we sampled the next largest individual tree from that species. If three trees were not available in the chosen plot, additional individuals of the same species nearby were sampled. Leaf samples from one fully sunlit canopy branch (of at least 1 cm diameter) were taken from selected trees. In addition, fully shaded canopy leaves were collected from a fraction of the same trees. From each branch, five leaves from simple-leaved species, or five individual leaflets from compound-leaved species (both referred to as 'leaf' below) were sampled for trait measurements. In the case of compound leaves, the entire compound leaf was also collected for whole-leaf area calculations. Leaves were chosen with minimal damage (i.e. herbivory). Leaves were placed in coolers from the field plot to the field lab for drying at c. 50 °C, and thereafter stored in paper envelopes prior to analysis. The sample set analyzed for bulk leaf and n-alkanes includes 405 individual samples distributed across nine forest plots, including 129 species from 47 families, representing 18–73% of the forest population (Table 1), with n-alkane concentrations reported in Feakins et al. (2016b). A smaller subset of leaf samples was analyzed for n-alkanoic acid $\delta^{13}C$ (76 individuals, 29 species, 22 families) for a sample set where plant water and leaf wax concentrations and hydrogen isotopic compositions of n-alkanes and n-alkanoic acids have been reported (Feakins et al., 2016a).

2.4. Lipid extraction and compound identification and quantification

The dried leaves were cut using solvent-cleaned scissors, and leaf waxes were subsequently extracted by immersing the leaf three times with dichloromethane (DCM):methanol (MeOH) 9:1 v/v using a Pasteur pipette. The lipid extract was separated into neutral and acid fractions by column chromatography through LC-NH$_2$ gel, using 2:1 DCM:isopropanol (5 mL) and 4% formic acid in diethyl ether (5 mL) respectively. The neutral fraction was separated by column chromatography through 5% water-deactivated silica gel by hexane, DCM and MeOH (5 mL each). The n-alkanes were eluted with hexane. The n-alkanoic acids, which are contained in the acid fraction, were methylated into fatty acid methyl esters (FAMEs) using MeOH of known isotopic composition with 5% hydrochloric acid at 70 °C for 12 h. MilliQ water was then added to the product, which was then partitioned into hexane. The hexane extract was further separated through silica gel column chromatography by eluting hexane and DCM (5 mL each), the latter fraction containing the FAMEs. Purified n-alkane and FAME samples were then dissolved in hexane for compound identification, quantification, and isotopic measurements.

2.5. Compound-specific carbon isotopic analysis

Carbon isotopic composition ($\delta^{13}C$) of individual odd chain n-alkane and even chain n-alkanoic acid compounds (C_{27} to C_{33} and C_{22} to C_{32} respectively) were measured using gas chromatography isotopic ratio mass spectrometry (GC-IRMS; Thermo Scientific Trace gas chromatograph connected to a Delta V Plus mass spectrometer via an Isolink combustion furnace at 1000 °C) at the University of Southern California. We checked the linearity in $\delta^{13}C$ determination across a range of peak amplitude (1–10 V) daily, with standard deviations averaging 0.06‰. Only the compounds with peak amplitudes within this dynamic range were accepted. $\delta^{13}C$ values of target peaks were normalized to the Vienna Pee Dee Belemnite (VPDB) standard by comparing with an external standard containing 15 n-alkane compounds (C_{16} to C_{30}), with $\delta^{13}C$ values ranging from −33.3 to −28.6‰, obtained from A. Schimmelmann, Indiana University, Bloomington. The external standard was analyzed at least twice a day through the course of the analysis, and the root-mean-square error (RMSE) was on average 0.2‰. An internal standard (C_{34} n-alkane) was co-injected with some of the samples to check for stability through the course of the sequence. Samples were measured once with replicate precision for a subset averaging 0.08‰. The $\delta^{13}C$ values of the n-alkanoic acids were calculated from the $\delta^{13}C$ values of the corresponding FAMEs using $\delta^{13}C$ of the added methyl group by mass balance ($\delta^{13}C$ of methanol = −25.45 ± 0.37‰).

2.6. Bulk leaf carbon isotope analysis

Dried leaves were ground in a Wiley mill to a fine powder (20 mesh), packed in Sn capsules and combusted via an Elemental Analyzer (Costech Analytical Technologies Inc. Valencia, CA, USA) connected to a Picarro G2131-i cavity ring-down spectroscopy (CRDS) for determination of $\delta^{13}C_{leaf}$ values. Samples were normalized to the VPDB scale by comparison to a Peach NIST SRM 1547 standard (mean $\delta^{13}C$ = −25.96 ± 0.12‰). An internal reference standard (Lemon Tree Standard: mean $\delta^{13}C$ = −28.12 ± 0.11‰) was interspersed every 20 samples to monitor stability.

2.7. Carbon isotopic fractionation

We report isotopic fractionations between the substrate, e.g., atmospheric carbon dioxide, a, of carbon isotopic composition $\delta^{13}C_a$, and product, e.g., plant tissue, p, with $\delta^{13}C_p$, as enrichment factors ($\varepsilon_{p/a}$), calculated with the following equation following Hayes (1993):

$$\varepsilon_{p/a} = \alpha_{p/a} - 1 = [(\delta^{13}C_p + 1)/(\delta^{13}C_a + 1)] - 1 \qquad (2)$$

where $\delta^{13}C$ is in fractional notation, and $\varepsilon_{p/a}$ yields a negative number associated with the discrimination against $^{13}CO_2$ in plants. The capital delta symbol, Δ has been the convention in the plant carbon isotope biochemistry community following (Farquhar et al., 1989):

$$\Delta_{a/p} = \alpha_{a/p} - 1 = [(\delta^{13}C_a + 1)/(\delta^{13}C_p + 1)] - 1 \qquad (3)$$

where Δ is positive when plants discriminate against $^{13}CO_2$ whereas ε is negative. $\delta^{13}C$, ε and Δ are reported in per mil units (‰) which implies a factor of 1000 (Cohen et al., 2007). Here we report ε (by Eq. (2)) and provide a calculator in Appendix A for quick conversion to Δ.

Although not a product/substrate relationship, we also calculate the isotopic fractionation ($\varepsilon_{29alk/leaf}$) between $\delta^{13}C_{leaf}$ and $\delta^{13}C_{29alk}$, where:

$$\varepsilon_{29alk/leaf} = [(\delta^{13}C_{29alk} + 1)/(\delta^{13}C_{leaf} + 1)] - 1 \qquad (4)$$

after (Chikaraishi et al., 2004). $\delta^{13}C_{29alk}$ values are almost always lower than $\delta^{13}C_{leaf}$ resulting in $\varepsilon_{29alk/leaf}$ values that range from -15 to $+1$‰ ($n < 250$ plants; compiled by Diefendorf and Freimuth, 2017). There may be systematic differences based on plant biology (Diefendorf and Freimuth, 2017) or climate (Freeman and Pancost, 2014), however inferences remain tentative given limited sample sizes for biomarkers.

2.8. Community average

Average values for each 1-ha forest plot were estimated using both the unweighted mean of all sampled individuals and community-weighted mean. The community-weighted mean (cwm) and uncertainty (σ_w) were calculated as follows:

$$cwm = \frac{\sum_{i=1}^{n}(x_i \times w_i)}{\sum_{i=1}^{n} w_i} \qquad (5)$$

$$\sigma_w = \sqrt{\frac{\sum_{i=1}^{n} w_i \times (x_i - cwm)^2}{\sum_{i=1}^{n} w_i}} \qquad (6)$$

where n is the number of species weighted, w_i is the weight (concentration of the individual leaf wax compound, if appropriate, and species basal area), and x_i is trait value for the ith species. Eq. (6) accounts for interspecific variations, but does not propagate intraspecific variability.
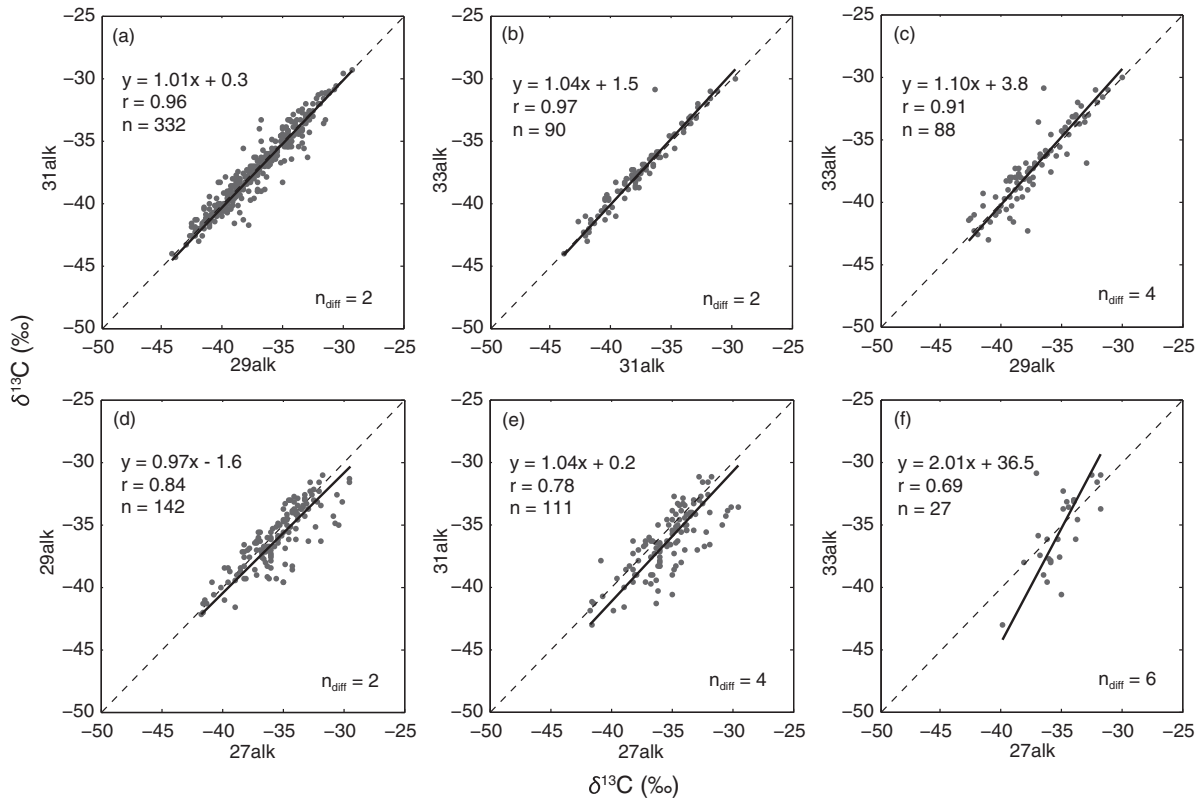

Fig. 2. Crossplots of $\delta^{13}C_{wax}$ values between odd-chain n-alkane homologues measured from individual sunlit canopy leaf samples, showing (a–c) comparison among C_{29}, C_{31} and C_{33}; (d–f) C_{27} compared with other chain lengths. Black lines indicate orthogonal distance regressions (all with $p < 0.0001$). Dashes show the 1:1 lines. n_{diff} indicates the difference in chain lengths between the compounds displayed.

3. RESULTS

3.1. Leaf wax δ^{13}C results

We report δ^{13}C values for n-alkanes from 405 sunlit canopy leaf samples covering 129 species from all nine sites, as well as n-alkanoic acids from 76 samples covering 29 species from five of the nine sites (see Supplementary Information for results and discussions of n-alkanoic acids). We additionally sampled 65 shaded canopy leaf samples, and 11 understory leaves (from ESP-01). Production of different compounds and homologues varies between species. Thus, we report δ^{13}C measurements from C_{27}, C_{29}, C_{31} and C_{33} n-alkanes where those individual compounds are present in sufficient concentrations for isotopic determination. We observe strong orthogonal distance regressions ($r > 0.9$) among δ^{13}C values of C_{29}, C_{31} and C_{33} n-alkanes, close to the 1:1 line (Fig. 2a–c). The C_{27} n-alkane yields weaker orthogonal distance regressions with other homologues ($r = 0.69$–0.84; Fig. 2d–f), that are significantly offset from the 1:1 line by Student's t-test, on average by $+0.7 \pm 1.5‰$ (relative to C_{29}) and $+1.2 \pm 1.8‰$ (relative to C_{31}; 1σ; $p < 0.01$). This may be analytical artefact, as C_{27} is generally of lower concentration.

3.2. Leaf wax δ^{13}C values across the elevation profile

To investigate the altitudinal trend, we survey $\delta^{13}C_{wax}$ values in sunlit, upper canopy leaves. δ^{13}C values of C_{29} n-alkane (the dominant chain length; Feakins et al., 2016b) from individual leaf samples range from -44.1 to $-29.2‰$ across all sites. Despite $\sim$10‰ variability between individuals within each site, we observe a trend toward higher $\delta^{13}C_{29alk}$ as elevation increases (Fig. 3). The elevation trends are similar among homologues (not illustrated).

Our sampling for n-alkanes represents 18–73% of the total basal area for each of the nine 1 ha forest plots (Table 1). We calculated site mean traits based on the unweighted means of the individuals (Table 2). We also calculated the community-weighted mean, where species mean values are weighted by wax abundance and species basal area (by Eq. (5); see Appendix A for individual, species-level and site-level results). For $\delta^{13}C_{29alk}$, unweighted and community-weighted site mean values differ by $\leq 1‰$ (Fig. 3) and they produce a strong $\delta^{13}C_{29alk}$-elevation correlation with similar gradients. Species-mean alkane concentrations are not well determined from sample sizes of three to five leaves given the large intra-species variability (Feakins et al., 2016b). The community weighting introduces large uncertainty with poorly-constrained species-mean alkane concentrations. Therefore, we continue only with discussion of the unweighted mean values as the best central estimates, similar to Feakins et al. (2016b) and Asner et al. (2016).

We find an increasing trend in $\delta^{13}C_{29alk}$ with elevation from unweighted site mean values of $-39.1‰$ at 215 m to $-34.2‰$ at 3.5 km, an increase of 5‰. Linear regression of $\delta^{13}C_{29alk}$ with elevation yields a slope of $+1.45 \pm 0.33‰$ km^{-1} (95% CI; $r^2 = 0.94$, $p < 0.01$; Fig. 3) and
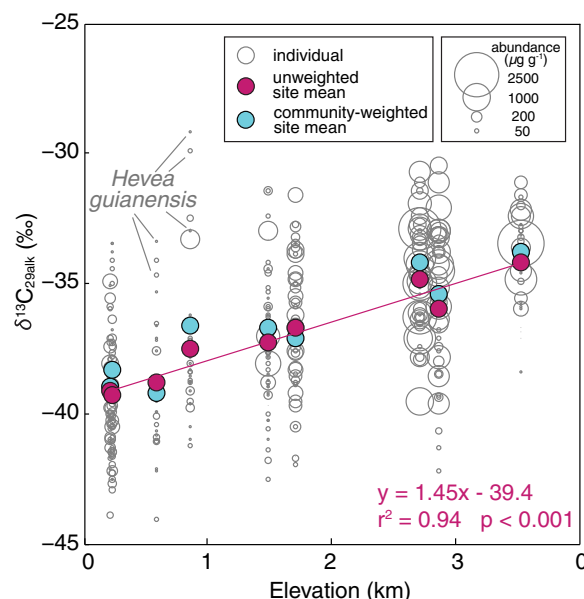

Fig. 3. δ^{13}C values of C_{29} n-alkane from sunlit canopy leaf samples versus elevation. Grey open circles indicate individual data with sizes scaled to leaf wax abundance. Also showing unweighted mean (pink circles), and community-weighted mean (blue circles) for each site, and ordinary least squares linear regression of the unweighted site means (pink line). *Hevea guianensis* (rubber tree) has anomalously high δ^{13}C values (included in site-mean). (For interpretation of the references to color in this figure legend, the reader is referred to the web version of this article.)

projected $\delta^{13}C_{29alk}$ at sea level (intercept) of $-39.4 \pm 0.6‰$ (95% CI). To our knowledge this is the first time that such an elevation response has been demonstrated in the carbon isotopic composition of leaf wax biomarkers in living plants, let alone for a large number of samples in humid tropical forests.

3.2.1. Taxon-specific leaf wax δ^{13}C gradients

The elevation trends reported above represent the average of all sampled canopy tree species (angiosperms). Due to the high turnover in the tree species community, we were unable to follow a single species across the environmental gradient. One genus, *Ocotea*, has a broad geographic range (0.215–2.719 km), with 19 sampled individuals (Fig. 4a), and four families (Clusiaceae, Euphorbiaceae, Lauraceae, Rubiaceae) span a wide range of elevation (Fig. 4b). Within these wide-spread taxa, some species display offsets from the site mean values. For example, *Hevea guianensis* (rubber tree), present at PAN-02 and PAN-03, is significantly ^{13}C-enriched relative to other Euphorbiaceae by Student's t test, and c. 5‰ heavier than site mean values (Fig. 3), perhaps due to its latex production, explaining the lack of elevation trend among Euphorbiaceae. All other taxonomic groups, show increasing $\delta^{13}C_{29alk}$ with elevation (Fig. 4; similar patterns are found for $\delta^{13}C_{leaf}$, not illustrated), but small sample sizes increase uncertainties (see Section 4.3). These findings suggest that taxonomic turnover does not determine the altitude effect; but in the context of a natural tran-

Table 2
Unweighted site-mean carbon isotopic compositions and fractionations in the Andes-Amazon transect.

Site summary data					Leaf wax biomarker (‰)						Bulk leaf (‰)					
Site	Elev. (km)	pCO_2 (ppmv)	MAP (mm)	n spl.	$\delta^{13}C_{29alk}$	se	$\varepsilon_{29alk/CO2}$	se	$\varepsilon_{29alk/leaf}$	se	$\delta^{13}C_{leaf}$	se	$\varepsilon_{leaf/CO2}$	se	$\Delta_{leaf/CO2}$	se
TAM-06	0.215	389	1900	38	−39.1	0.3	−31.0	0.3	−8.2	0.3	−31.1	0.3	−22.9	0.3	23.5	0.3
TAM-05	0.223	389	1900	58	−39.3	0.3	−31.2	0.3	−8.2	0.3	−31.4	0.2	−23.2	0.2	23.7	0.2
PAN-02	0.595	372	2366	25	−38.8	0.5	−30.7	0.5	−8.1	0.5	−30.9	0.2	−22.7	0.2	23.3	0.2
PAN-03	0.859	361	2835	36	−37.5	0.5	−29.3	0.5	−7.5	0.4	−30.2	0.3	−21.9	0.3	22.4	0.3
SPD-02	1.494	335	5302	57	−37.3	0.3	−29.1	0.3	−7.6	0.3	−29.8	0.2	−21.6	0.2	22.1	0.2
SPD-01	1.713	327	5302	58	−36.7	0.3	−28.6	0.3	−7.3	0.2	−29.7	0.2	−21.4	0.2	21.9	0.2
TRU-04	2.719	291	2318	49	−34.8	0.3	−26.6	0.3	−6.1	0.3	−28.8	0.3	−20.6	0.3	21.0	0.3
ESP-01	2.868	286	1560	44	−36.0	0.4	−27.8	0.4	−7.5	0.3	−28.7	0.3	−20.4	0.3	20.9	0.3
ACJ-01	3.537	265	1980	40	−34.2	0.3	−26.0	0.3	−5.9	0.2	−28.5	0.1	−20.3	0.2	20.7	0.2

pCO_2 (ppmv) is an equivalent value determined based on elevation, with sea level pCO_2 taken at 394 ppm (1-year average prior to August 2013 sampling; Keeling et al. (2001), with 5 ppmv added to reflect the higher CO_2 concentrations in the Amazon canopy compared to the free atmosphere (Olsen and Randerson, 2004). Showing unweighted site mean and standard errors. n spl. = number of samples. All other abbreviations as in the text.

sect with high turnover, it remains untestable whether elevation response is driven by species turnover.

3.3. Comparison of leaf wax and bulk leaf $\delta^{13}C$

Comparing $\delta^{13}C$ values of leaf wax and bulk leaf for the same tree (different branches), we find a linear correlation between $\delta^{13}C_{leaf}$ and $\delta^{13}C_{29alk}$ ($y = 1.95x − 21.3$, $r = 0.68$, $n = 399$, $p < 0.01$), as well as with other chain lengths (Fig. 5a). The comparison between $\varepsilon_{wax/leaf}$ values for different chain lengths of n-alkanes are reported in Fig. 5b and Appendix A. We focus on the C_{29} n-alkane (the dominant homologue; Feakins et al., 2016b) vs. the bulk leaf (comprised of many biochemicals) in order to evaluate the isotope systematics in individual leaf wax compounds. The mean carbon isotopic fractionation between leaf wax C_{29} n-alkane and bulk leaf ($\varepsilon_{29alk/leaf}$) is $−7.4 \pm 2.2$‰ (1σ, $n = 399$) across all samples (Fig. 5b). We however find a reduction in $\varepsilon_{29alk/leaf}$ with increasing elevation (slope $= 0.60 \pm 0.30$‰ km^{-1}, 95% CI, $r^2 = 0.76$, $p < 0.01$; Fig. 6b), as the elevational gradient in $\delta^{13}C_{29alk}$ is significantly steeper than that in $\delta^{13}C_{leaf}$ ($+1.45 \pm 0.33$ and $+0.87 \pm 0.16$‰ km^{-1} respectively; 95% CI; Fig. 6a). $\varepsilon_{29alk/leaf}$ ranges from $−5.9 \pm 1.5$‰ (1σ, $n = 40$) at the highest site (ACJ-01) to $−8.2 \pm 1.6$‰ (1σ, $n = 38$) at the lowest site (TAM-06). Using the linear regression calculated here, the projected $\varepsilon_{29alk/leaf}$ at sea level is $−8.3 \pm 0.6$‰ (95% CI; Fig. 6b).

3.4. Canopy effects

3.4.1. Sunlit versus shaded canopy leaves

To test whether light intensity affects $\delta^{13}C_{wax}$ values, we calculated the $\delta^{13}C$ offsets between paired sunlit and shaded leaves ($\varepsilon_{sun/shade}$) for the bulk leaf, C_{29} n-alkane, and $\varepsilon_{29alk/leaf}$ (Fig. 7a). Sunlit leaves are on average ^{13}C-enriched in C_{29} n-alkane relative to shaded leaves, but the average difference is small (0.8 ± 2.3‰, 1σ; $n = 62$) relative to the very large range of observations for sunlit ($1\sigma = 2.9$‰, $n = 405$) and shaded leaves ($1\sigma = 2.9$‰, $n = 65$). The sun/shade enrichment is more evident in the bulk leaf, which shows a larger mean $\varepsilon_{sun/shade}$ of 1.3 ± 1.3‰ (1σ, $n = 57$), with a narrower distribution for sunlit ($1\sigma = 1.8$‰, $n = 405$) and for shaded ($1\sigma = 1.6$‰, $n = 65$) leaves. $\varepsilon_{sun/shade}$ for both measures of $\delta^{13}C$ values are significantly below zero by Student's t-test ($p < 0.01$). In contrast, $\varepsilon_{29alk/leaf}$ shows no differences between sunlit and shaded leaves (Fig. 7a).

3.4.2. Canopy versus understory

Although this study focuses on sampling the dominant production of leaves in the canopy, we compare a small number of understory plants (10 samples, five species) collected at ESP-01 with canopy leaves (Fig. 7b). $\delta^{13}C_{29alk}$ values of leaves on understory shrubs range from $−44.4$ to $−35.3$‰, averaging $−38.4 \pm 2.5$‰ (1σ, $n = 10$). In comparison, $\delta^{13}C_{29alk}$ of the sunlit canopy leaves from trees span $−42.2$ to $−30.5$‰ and averaging $−36.0 \pm 2.8$‰ (1σ, $n = 43$), and hence significantly enriched ($p = 0.013$) relative to understory leaves.
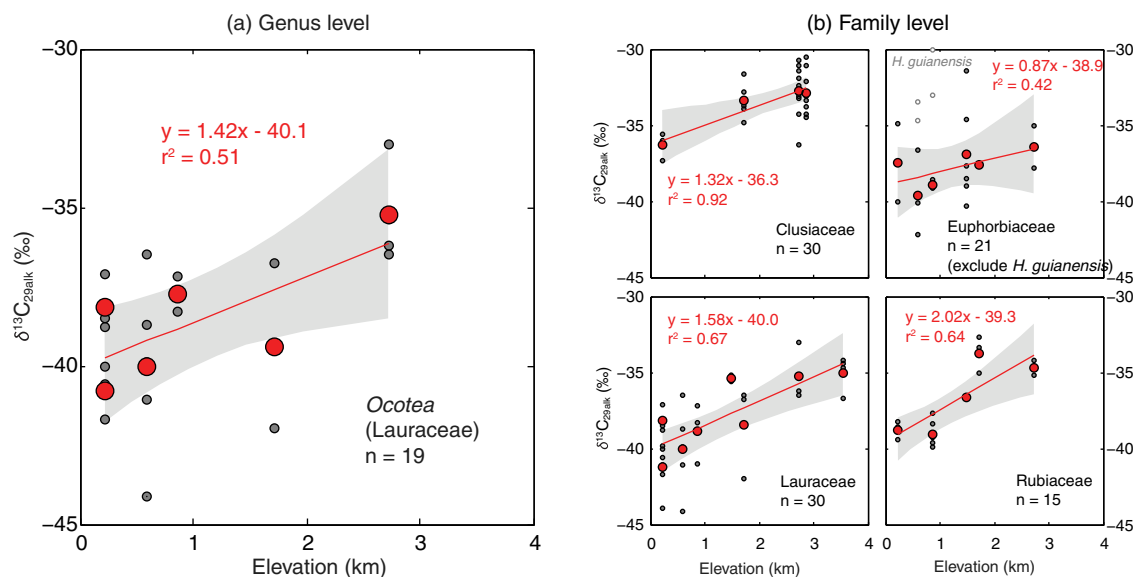
Fig. 4. Elevation trends in $\delta^{13}C_{29alk}$ from the same (a) genus (*Ocotea*) and (b) families that span a wide range of elevations (grey: individual samples, red: unweighted site means). All elevation trends are significant ($p < 0.01$) based on the individual samples, except for Euphorbiaceae ($p = 0.18$ excluding *H. guianensis*). (For interpretation of the references to color in this figure legend, the reader is referred to the web version of this article.)
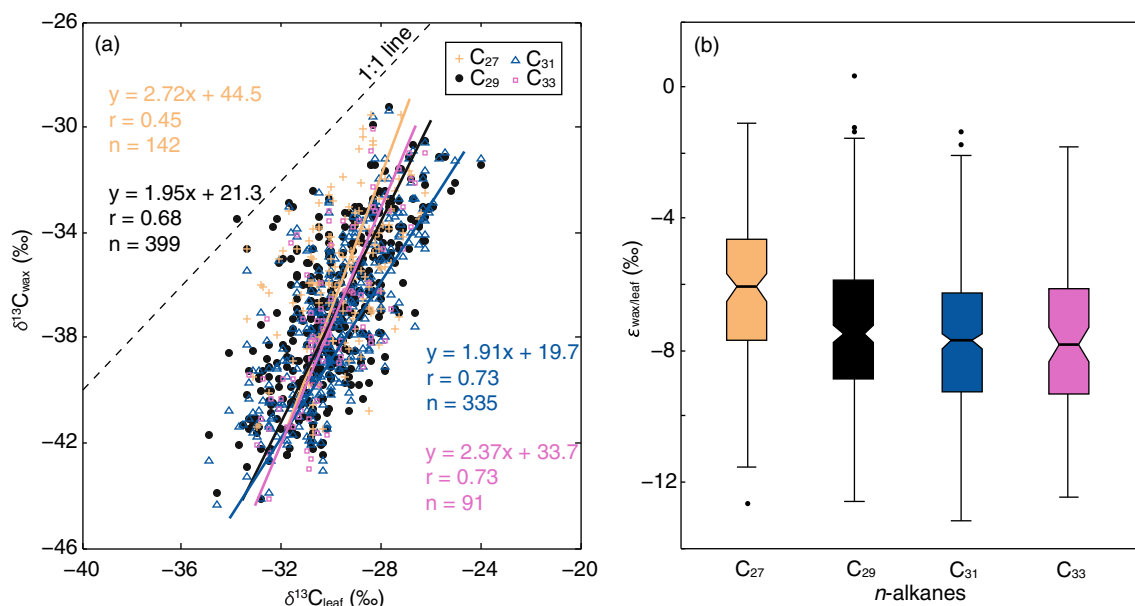

Fig. 5. Comparison of $\delta^{13}C$ values between *n*-alkane homologues and bulk leaf, showing (a) scatter plot of individual samples and orthogonal distance regressions (all with $p < 0.001$); (b) notched box and whisker plots representing distributions of $\varepsilon_{wax/leaf}$ values of different *n*-alkane homologues (horizontal black lines: median; boxes: upper and lower quartile; whiskers: 5th and 95th percentile; dots: data beyond 5th and 95th percentile). Data are from individual sunlit leaf samples from all sites.

4. DISCUSSIONS

4.1. Comparison of leaf wax and bulk leaf properties

We measured bulk and compound specific carbon isotopic compositions on leaves on the same trees. The average $\varepsilon_{29alk/leaf}$ ($-7.4 \pm 2.2‰$, 1σ, $n = 399$; Fig. 5b) across all sam-

ples is similar to values previously reported from eastern Africa ($-7.4 \pm 2.1‰$, 1σ, $n = 48$; Magill et al., 2013) and southern Alberta ($-7.2 \pm 0.9‰$, 1σ, $n = 15$; Conte et al., 2003), and larger than that compiled elsewhere ($-5.2 \pm 2.4‰$, $n = 109$ for all environments; $-5.5 \pm 2.5‰$, $n = 74$ for tropical and subtropical climates; Diefendorf and Freimuth, 2017). Differences between study averages

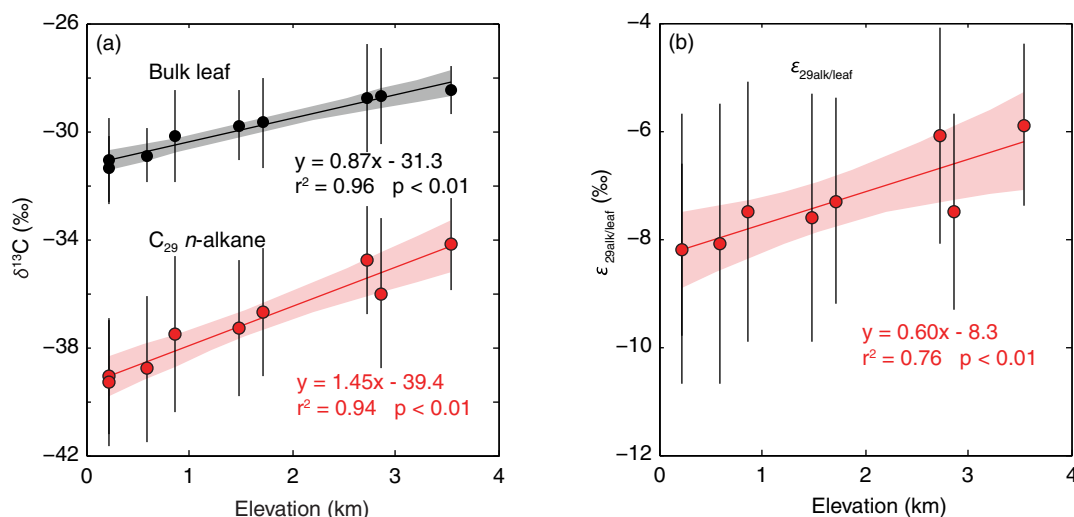Fig. 6. Elevation trends in (a) bulk leaf (black) and $\delta^{13}C$ of C_{29} n-alkane (red), and (b) $\varepsilon_{29alk/leaf}$ (red), showing unweighted site-means (circles), 1σ (error bars), and linear regressions (lines) and 95% confidence intervals (shading). (For interpretation of the references to color in this figure legend, the reader is referred to the web version of this article.)
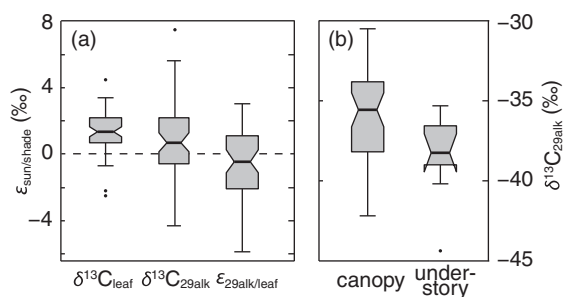

Fig. 7. (a) Carbon isotopic offset between paired sunlit and shaded leaf samples ($\varepsilon_{sun/shade}$) from the same tree, for $\delta^{13}C_{leaf}$ ($n = 57$), $\delta^{13}C_{29alk}$ ($n = 62$), and $\varepsilon_{29alk/leaf}$ ($n = 54$). The first two distributions are significantly ($p < 0.01$) above zero (dashed line) indicating sunlit leaves are enriched relative to shaded leaves, whereas the third distribution is not significantly offset from zero at 95% confidence level. (b) Comparison of $\delta^{13}C_{29alk}$ values of sunlit canopy leaves ($n = 43$) and understory leaves ($n = 10$) at ESP-01. The two distributions are different at 95% level ($p = 0.013$). Notched box and whisker plots show median (horizontal lines), low and upper quartiles (boxes), 5th and 95th percentiles (whiskers), and data beyond 5th and 95th percentiles (dots).

may be due to plant life form (Diefendorf and Freimuth, 2017) and/or climate (Freeman and Pancost, 2014). Here we add considerably to the data on tropical C_3 trees. Within our dataset, we find larger fractionations in the lowland rainforest, and smaller fractionations in montane forests. The systematic trend in $\varepsilon_{29alk/leaf}$ with elevation (Fig. 6b), means that the extrapolated sea-level fractionation ($-8.3 \pm 0.6‰$; 95% CI) may be more appropriate than the overall mean for application in future tropical lowland studies. However, we caution that only 46% of variability of $\delta^{13}C_{29alk}$ is explained by the observed variability in $\delta^{13}C_{leaf}$ (Fig. 5a) such that we do not recommend relying heavily on

of bulk leaf observations in the interpretation of leaf wax biomarker records.

We emphasize that $\varepsilon_{29alk/leaf}$ represents the offset of a specific compound relative to the entire leaf and is not a direct biosynthetic precursor-to-product step. The offset may reflect multiple isotope effects, including changes in the magnitude of the fractionation as well as the proportions of biochemicals in the leaves, each of which may vary with species and climatie. Several aspects of foliar physiology and biochemistry change upslope, including decreases in cellulose and lignin, increases in LMA (leaf mass per area), soluble C (sugars), phosphorus (Asner et al., 2014b, 2016) and n-alkane concentrations (Feakins et al., 2016b). We tested whether thicker leaves (higher LMA) would reduce diffusion through the mesophyll cells and cause greater ^{13}C-enrichment, as previously reported in a single species (Vitousek et al., 1990). We found a weak positive correlation between LMA and $\delta^{13}C_{leaf}$ ($r = 0.45$, $p < 0.01$) and $\delta^{13}C_{29alk}$ ($r = 0.31$, $p < 0.01$), suggesting ^{13}C-enrichment in thicker leaves corroborating with the previous study (Vitousek et al., 1990). We observe no relationship between $\varepsilon_{29alk/leaf}$ and LMA, as well as phosphorous and lignin concentrations, suggesting these leaf trait changes are not responsible for the gradient in $\varepsilon_{29alk/leaf}$. We find weak correlations between $\varepsilon_{29alk/leaf}$ and concentrations of cellulose ($r = -0.12$, $p = 0.02$), soluble C ($r = 0.10$, $p = 0.04$), and n-alkanes ($r = 0.22$, $p < 0.01$). The latter suggests that the pool of precursor may have been used more completely when making waxier leaves. Similarly, a decrease in the $\delta^{13}C$ offset between bulk leaf and leaf wax was noted elsewhere as total wax concentration increased (Zhou et al., 2015). Here, these relationships only account for a small portion of the variance, with unexplained variance likely due to multiple variables in leaf physiology and biochemistry that are not readily quantified at the leaf level.

4.2. Environmental variables affecting carbon isotope fractionation

4.2.1. Irradiance and canopy closure

Sunlit leaves are ^{13}C-enriched relative to shaded leaves in both bulk leaf and leaf wax (Fig. 7a) suggesting influences from light intensity. Our results agree with previous theoretical and experimental studies on bulk leaf (Farquhar et al., 1989) and leaf waxes (Graham et al., 2014). ^{13}C-enrichment in sunlit leaves reflects a decrease in c_i/c_a likely brought about by a higher photosynthetic rate (Farquhar et al., 1989); an alternate possibility of lower stomatal conductance is unlikely in this wet climate (Table 1) and is not supported by leaf water isotopic evidence that indicates open exchange with the atmosphere (Feakins et al., 2016a). Leaf physiology may contribute as sunlit leaves tend to be thicker (mean $20 \pm 18.5\%$ higher LMA) than shaded leaves, and this may restrict diffusion of CO_2 into mesophyll cells. We find the sun/shade difference ($\varepsilon_{sun/shade}$) for $\delta^{13}C_{leaf}$ is positively correlated with the sun/shade LMA ratio ($r^2 = 0.33$, $p < 0.01$) such that leaf thickness may explain 33% of the ^{13}C-enrichment in the bulk leaf; but no significant correlation is observed for leaf wax. In addition, we find no significant sun/shade difference in $\varepsilon_{29alk/leaf}$, and thus infer light intensity exerts no effect on ^{13}C fractionation during wax biosynthesis, but leaf waxes preserve the sun/shade signature of the original photosynthate.

We sampled the understory at a single site ESP-01 and observed ^{13}C-depletion relative to the canopy (Fig. 7b). This is expected due to lower light intensities, and accumulation of ^{13}C-depleted respired CO_2 under the dense closed canopy (Cerling et al., 2011). Similar canopy effects have been observed in vertical canopy profiles in Panama, and that study concluded that upper canopy leaves are the most relevant for geological archives given their greater productivity (Graham et al., 2014). In contrast, individual tree height effects have been noted in other studies, typically showing an increase in $\delta^{13}C$ with increasing tree height within single forest plots for a variety of biochemical and physiological reasons (McDowell et al., 2011; Kenzo et al., 2015). Here, we do find a weak but significant positive correlation ($r^2 < 0.3$; $p < 0.05$) between tree height and $\delta^{13}C$ at some individual sites (lowland site TAM-06 for the C_{29} n-alkanes only; lowland to mid-elevation sites TAM-06 to SPD-02 for bulk leaf). At the landscape scale, tree height increases toward lower elevations (Table 1), but canopy $\delta^{13}C$ decreases (Fig. 6a), which means that plot-altitude effects (not tree height) dominate here.

4.2.2. Dual C and H isotopic analyses: insights into leaf-atmosphere exchange

In dry environments, where stomata regulate water loss, they can also be a driver of carbon dioxide limitation and thus ^{13}C-enrichment in both bulk leaf and leaf waxes. Water is not thought to be limiting in these humid tropical forests with high relative humidity ($>90\%$) and precipitation (>1.5 m yr^{-1}), and it has already been shown that leaf water content is minimally D- and ^{18}O-enriched in these trees (Feakins et al., 2016a). Thus, we do not expect to

see signs of restricted stomatal conductance, but we test this by comparing the C_{29} n-alkane hydrogen isotopic compositions (δD_{29alk}) measured from five study sites (Feakins et al., 2016a) to $\delta^{13}C_{29alk}$ reported for the same samples here – the dual isotope measurements were made on the same aliquots from the same leaves. To parse similar climatic and elevation zones, we divide the sites into three groups: the wettest, mid-elevation montane sites SPD-01 and SPD-02, the lowland sites TAM-05 and TAM-06, and the upper site ESP-01. We see no relationship between $\delta^{13}C_{29alk}$ and δD_{29alk} at all sites (Fig. 8), suggesting water limitation is not an effect on carbon isotope fractionations in these tropical forests.

4.2.3. Adiabatic controls on carbon isotope fractionation

Adiabatic changes with elevation imply that the pressure of the atmosphere, as well as all component gases, decreases with elevation in a very predictable manner. Changes that may be relevant to plant growth include adiabatic declines in pCO_2, pO_2, total pressure, temperature and humidity (in addition to local climatic or ecological variables). Plants respond to these multiple changes physiologically and biochemically, and the adiabatic processes may be encoded in their leaf $\delta^{13}C$, but the driving mechanism are confounded (Körner, 2007). Experimental studies can help to isolate a single process. We compare the elevation-based evidence, converted to pCO_2 equivalency (by Eq. (2)) from this study for trees in a very wet, tropical climate with evidence from Schubert and Jahren (2012) for forbs grown under controlled moisture and pCO_2 'fertilization' experiments in the laboratory reporting $\delta^{13}C$ for both bulk and C_{31} n-alkanes (Fig. 9). After converting the decline in partial pressure to ppmv equivalent units and fitting with a linear regression, we find the Peruvian transect to be consistent but offset from the predicted slope of the hyperbolic curve at lower pCO_2, beyond the range of the earlier empirical work. While experimentation allows the implications of variations in pCO_2 to be isolated from other variables (CO_2 explains about 30% of the measured variance),
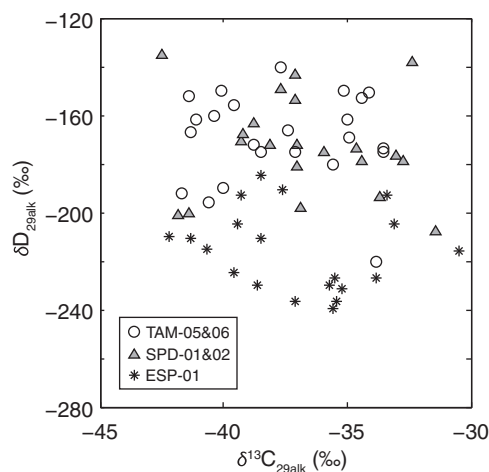

Fig. 8. Comparison between C_{29} n-alkane $\delta^{13}C$ (from this study) and δD (Feakins et al., 2016b). There is no significant correlation.
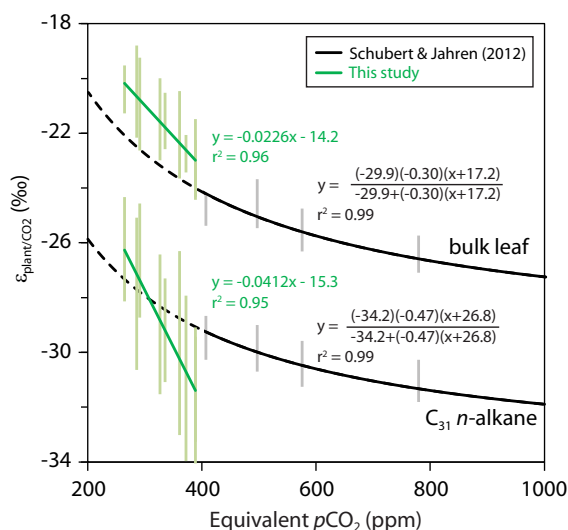
Fig. 9. Comparing the relationship between pCO_2 and carbon isotopic fractionation from the Perú transect (green; this study) to growth chamber experiments (black; recalculated from Schubert and Jahren, 2012) with 1σ (error bars). Equivalent pCO_2 for the Perú transect is determined based on elevation (see Eq. (2)), with sea level pCO_2 taken at 394 ppmv, the 1-year average prior to August 2013 sampling (Keeling et al., 2001).

experimental findings have been dismissed as short-term responses that may be masked by plant adaptation in natural ecosystems (Kohn, 2016). Our transect follows experimental predictions with an apparent response of plant $\delta^{13}C$ to low pCO_2 (200–400 ppmv) in a tropical elevation transect with fully-grown C_3 trees (Fig. 9). But, growth experiments should test the mechanism at low pCO_2.

Competing hypotheses include the role of the pO_2 decline with elevation, which would act to suppress photorespiration and increase photosynthesis efficiency (Berner et al., 2000). Few growth experiments have studied the effect of pO_2 on plant ^{13}C-discrimination relevant to high altitude. A growth experiment with *Phaseolus vulgaris* at 15% O_2 found $\delta^{13}C_{leaf}$ values were +2.1‰ higher than plants grown at ambient conditions, or 21% O_2 (Beerling et al., 2002). While the negative correlation between pO_2 and $\delta^{13}C$ means this is a competing mechanism, the isotope effect would have to be stronger than determined by experiments to explain the magnitude of the observed shift across the elevation profile. Furthermore, at altitude the O_2/CO_2 ratio does not change and it is this ratio that is predicted to control photorespiration from first principles (Beerling et al., 2002).

Each of the experimental studies selectively enrich the atmosphere in either pO_2 or pCO_2. As CO_2 and O_2 are mutually competitive inhibitors at their binding sites on RuBisCO, plants may be responding to the changing partial pressure of either gas or to the changing O_2/CO_2 mixing ratio in each of the laboratory experiments (Beerling et al., 2002). But, either the O_2 or CO_2 mechanism must dominate, as the pO_2/pCO_2 is unchanged adiabatically. Körner (2007) suggests that plants make biochemical adap-

tations to use CO_2 more efficiently at high altitude, just as animals increase ventilation to adapt to lower O_2.

Adiabatic effects also determine the monotonic decline in temperature with altitude. However elsewhere the effects of low temperature have been suggested to be minimal based on cold-tolerant, Arctic species that showed a response of $\delta^{13}C$ to elevation in the Alps, but minimal response to low temperatures (Zhu et al., 2010). Theoretical predictions that the decline in absolute air pressure and humidity would aid diffusivity of CO_2 into the leaf (Terashima et al., 1995) should increase selection against ^{13}C and thus cannot explain ^{13}C-enrichment at altitude. Instead, various leaf physiological changes that inhibit diffusion between stomata and carboxylation sites (Vitousek et al., 1990) are more likely to work in the direction of the observed effect (discussed in Section 4.1). The mechanism must remain unresolved as we cannot separate multiple variables (adiabatic changes and taxonomic turnover), but the net effect observed in our finding of ^{13}C-enrichment with elevation is consistent with pCO_2 theory.

4.3. Altitude effect on plant wax $\delta^{13}C$

4.3.1. Evaluating robustness of the altitude effect

The large inter- and intra-species variability of plant $\delta^{13}C$ values has previously been raised as a concern for resolving environmental responses in the past as well as presenting challenges for adequate representation of population mean values in modern calibration studies. A previous study in a tropical closed-canopy forest used Monte Carlo resampling to find the number of leaves (50) from leaf litter required to robustly capture canopy closure given the low proportion of understory leaves (Graham et al., 2014). We used a similar Monte Carlo approach to evaluate the sampling required for a robust elevation regression. We randomly subsampled ($n = 1–50$) our $\delta^{13}C_{29alk}$ dataset from each of the nine sites (with replacement when $n >$ number of measured $\delta^{13}C_{29alk}$ data), and calculated the site means and linear regressions with elevation for 2000 iterations. Uncertainties increased as the number of samples per site decreases (Fig. 10a). These tests reveal that the sample size of our $\delta^{13}C_{29alk}$ dataset (n per site = 25–58) is sufficient to capture a robust regression; beyond $n = 20$ there is limited improvement and false negatives increase sharply for $n < 10$.

In order to generalize our findings, we generated a synthetic $\delta^{13}C_{29alk}$ dataset for the elevation profile and subsampled different numbers of evenly-spaced sites (n sites = 3–50) along the 3.3 km elevation transect with 2000 iterations. The synthetic dataset was defined to match the properties of the measured $\delta^{13}C_{29alk}$ (site mean values determined from the $\delta^{13}C_{29alk}$ regression with elevation; 10,000 individuals per site with a Gaussian distribution, $1\sigma = 2.4‰$, the transect average), and we repeated the analysis on 10 synthetic datasets. We found the number of sites are more important than the number of samples per site when seeking the minimum total sample size to obtain a robust regression of the population (Fig. 10b). For example, for a total sample size of 50, the chance of a statistically-significant elevation gradient (at the 95% confidence level) is highest when collecting
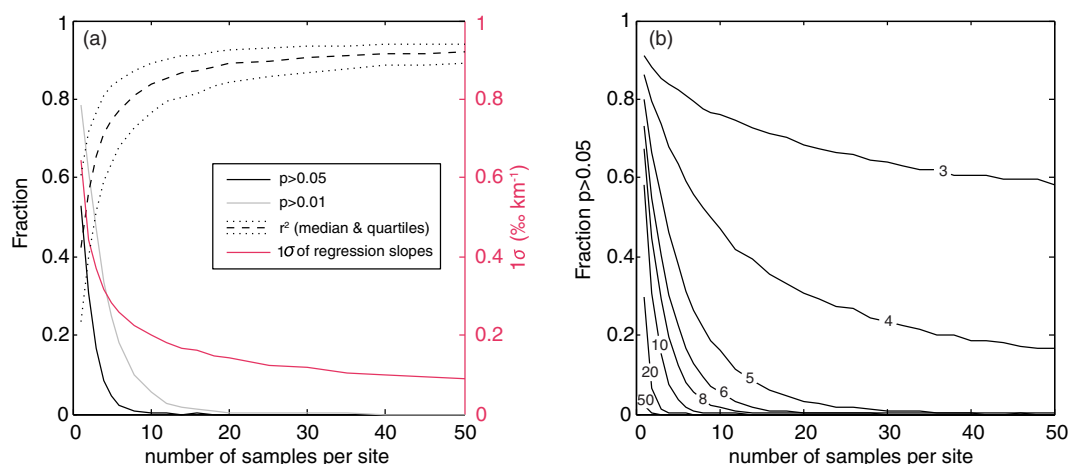
Fig. 10. Assessment of sensitivity of regression to sample size using a Monte Carlo subsampling approach (2000 iterations) (a) for different numbers of individuals per site from the measured $\delta^{13}C_{29alk}$ values at all nine study sites; and (b) for a synthetic $\delta^{13}C$ dataset matching the characteristics of the $\delta^{13}C_{29alk}$ dataset (mean 1σ distribution per site = 2.4‰, slope = 1.45‰ km^{-1}, RMSE of linear regression = 0.45‰) with different numbers of individuals per site (x axis) for different numbers of equally-spaced sites along a 3.3 km elevation transect (lines).

one sample each from 50 sites (Fraction$_{p>0.05}$ = 0.021), compared to 5 samples each from 10 sites (Fraction$_{p>0.05}$ = 0.037) and 10 samples each from 5 sites (Fraction$_{p>0.05}$ = 0.16). Our elevation transects for taxon-specific $\delta^{13}C_{29alk}$ (Fig. 4) and $\delta^{13}C_{30acid}$ subsets (Fig. S4) were based on 3–5 unevenly spaced sites, which have a high chance of a false negative (Fig. 10b).

4.3.2. Global synthesis

Although our study constitutes an unprecedented sample-size for the study of plant wax carbon isotope systematics in tropical forest ecosystems, it only considers data from one geographic region. Additional transect-based calibration efforts in other tropical forests, e.g. central Africa and southeast Asia, could be well-justified, given taxonomic differences may incur carbon isotope effects (e.g. *H. guianensis*, rubber tree), and given the high species diversity in the tropics (Kreft and Jetz, 2007; Ter Steege et al., 2010). Phylogenetic sampling schemes have indicated variations in carbon isotope fractionations between plant groups (Diefendorf et al., 2010, 2015). However, variations in precipitation amount are globally the dominant control on carbon isotope fractionations (Diefendorf et al., 2010), with the effect most apparent below ~1.5 m MAP. At higher MAP (above ~1.5 m), the effect becomes smaller because of the logarithmic relationship (Diefendorf et al., 2010). If carbon isotope fractionations are insensitive to precipitation amount in very wet climate regimes >1.5 m MAP, this allows other variables to be discerned. The western Amazon and Andean cloud forest regions included in this elevation transect have very high MAP (1.5–5.3 m) and relative humidity (75.2–93.7%; Table 1), and as expected, we find no correlation between $\delta^{13}C$ and MAP in our transect. We compile previously published data from locations with >1.5 m MAP in order to globally assess the altitude effects in very wet climates (Fig. 11). We find that the altitude effect identified in Perú is repeated in the global data com-

pilation in both bulk leaf (Fig. 11a) and leaf wax *n*-alkanes (Fig. 11b). Globally there is insufficient data to test this in the *n*-alkanoic acids. One limitation is the difference in data density across elevations (Fig. 11 insets), and our evidence for an altitude effect may perhaps encourage more data collection and reporting of data from altitudinal transects.

4.4. General significance

This large-scale study of carbon isotope systematics in tropical lowland and montane rainforests in Perú provides modern observational data to support tropical paleoenvironmental reconstructions. We characterize the bulk leaf and leaf wax $\delta^{13}C$ composition of tropical rainforest trees and demonstrate an altitude effect of *c.* +1‰ km^{-1} in this wet, forested gradient (Fig. 6) and find the pattern to be generalizable to other moist forests, based on a collation from the literature (Fig. 11). The sensitivity of site mean $\delta^{13}C$ values to elevation gain in the Andes Mountains (+4–6‰ gain from sea level to the tree line *c.* 4 km) is an order of magnitude greater than measurement uncertainties (*c.* 0.2‰), and although dwarfed by plant-to-plant variability (Fig. 3), with sufficient sample sizes (Fig. 10) the signals of elevation in site mean values clearly emerge in these humid forests.

4.4.1. Paleoaltimetry

Biomarker traits that are sensitive to elevation offer possibilities for reconstructing changes in elevation if preserved in suitable sedimentary archives, as well as differentiation of the source elevation of organic matter transported in rivers. Hydrogen isotopes in plant waxes (Polissar et al., 2009; Hren et al., 2010; Ernst et al., 2013; Ponton et al., 2014; Kar et al., 2016; Feakins et al., 2016a) and oxygen isotopes in carbonates (Poage and Chamberlain, 2001; Quade et al., 2011) each perform this function by recording the altitudinal gradient in isotopes in precipitation. In addition, the
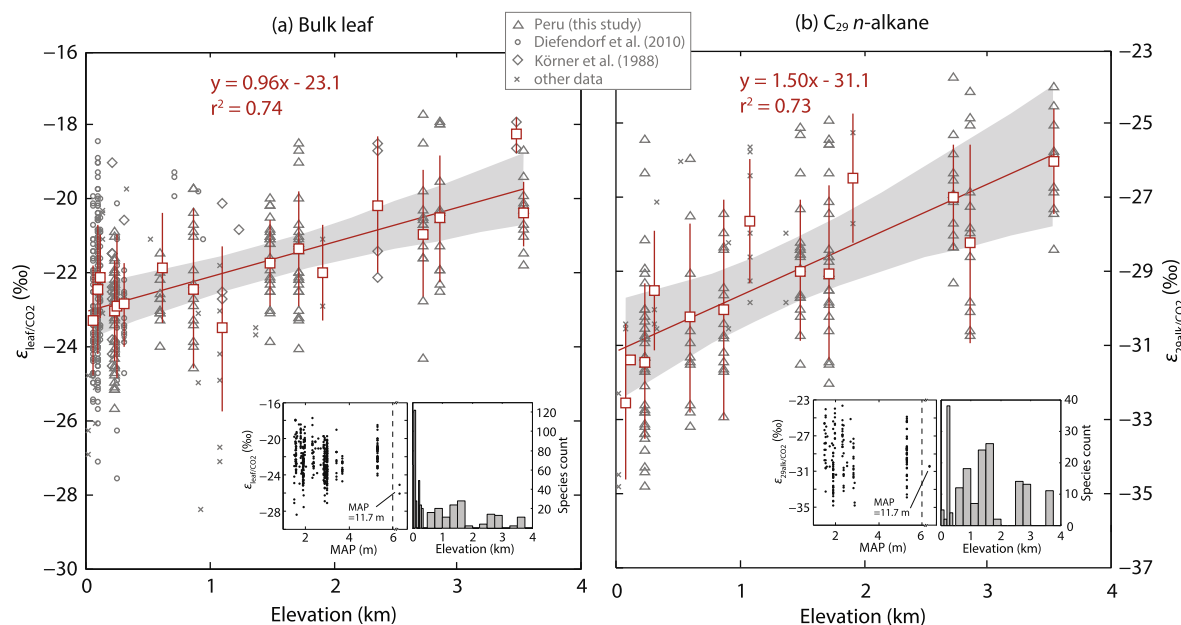
Fig. 11. Global elevation gradients in the carbon isotopic fractionations for (a) bulk leaf, $\varepsilon_{leaf/CO2}$ and (b) leaf wax C_{29} n-alkane, $\varepsilon_{29alk/CO2}$. Data (Appendix A) are from this study (triangles); Diefendorf et al. (2010) compilation (circles); Körner et al. (1988) compilation (diamonds); and other sources (crosses; Chikaraishi and Naraoka, 2003; Diefendorf et al., 2011; Vogts et al., 2009; Garcin et al., 2014). We only include data from angiosperm trees from locations with MAP > 1.5 m, to eliminate the aridity effect on $\delta^{13}C$ (see inset). Each individual data point (grey) represents a species which may come from a single measurement or an average from multiple samples. The number of samples, species at each site varies between studies and the coverage across elevations is also uneven (see inset). To account for the unevenness in data distribution, we plot elevation average data (red squares) and 1σ distribution (error bars), at increments of 50 m and 100 m for $\varepsilon_{leaf/CO2}$ and $\varepsilon_{29alk/CO2}$ respectively below 0.5 km, and 250 m increments above 0.5 km, with linear regression (red line) and 95% confidence interval (shading). Both elevation regressions are statistically significant ($p < 0.001$). (For interpretation of the references to color in this figure legend, the reader is referred to the web version of this article.)

'clumped' ^{13}C-^{18}O isotopic bond ordering in carbonates provides evidence for temperature (Ghosh and Brand, 2003; Huntington et al., 2010; Quade et al., 2013).

Paleoaltimetry with plant wax biomarkers has the potential to be based upon both the elevation response of δD_{wax} to precipitation δD (previously reported in this transect; Feakins et al., 2016a) and the adiabatic response of $\delta^{13}C_{wax}$ (demonstrated here) in humid tropical forests (Table 3). The main complications for these altitude proxies arise when shifting into dry climates. Aridity leads to closure of stomata to limit transpiration, with attendant ^{13}C-enrichment (Cernusak et al., 2013). Thus, $\delta^{13}C$ is confounded in profiles where aridity is a variable (Friend et al., 1989; Wei and Jia, 2009) but not in wet catchments, such as this one and that reported by Körner et al. (1991). The addition of another elevation-sensitive proxy, and especially the ability to measure two isotope systems ($\delta^{13}C$ and δD) in the same leaf wax molecules, offers the possibility to cross-check aridity effects (positive correlation) versus altitude effects (negative correlation). Uniquely the use of dual C and H isotopes should provide a convenient tracer of aridity effects as explained in Section 4.2.2. Here, both respond as altimeters.

4.4.2. Paleoecology

One common application of plant wax $\delta^{13}C$ values to lake or ocean sediment core reconstructions is to discern proportions of plants using the C_3 versus C_4 pathway (Schefuß et al., 2003; Castaneda et al., 2009; Feakins et al., 2013). Such studies may assume C_3 forests have a $\delta^{13}C_{29alk}$ of c. -38% as in the lowland sites here. Since contributions from high elevation sites may bias the sedimentary $\delta^{13}C$ record toward more enriched values, it would be important to rule out substantial high elevation contributions when attempting to reconstruct C_4 plant contributions to an otherwise C_3 ecosystem.

In fluvial studies, more ^{13}C-enriched values of plant waxes in transit have previously been interpreted as indicating C_4 plant inputs from the lowlands (Galy et al., 2011), or petrogenic inputs (Häggi et al., 2016), and each of these explanations is plausible. However, our data raise a third possibility, that contributions from upland ecosystems may also contribute a ^{13}C-enriched signal. This may be particularly relevant for interpretation of n-alkanes, which were identified as a more persistent and upstream component, versus n-alkanoic acids and n-alcohols which displayed a 'flashier' response with local inputs in the Congo River (Hemingway et al., 2016). Furthermore, higher elevation forests have been found to have higher concentrations of n-alkanes (Feakins et al., 2016b) and thus may represent a stronger source than lowland trees (Fig. 3).

In most cases C_4 interpretation are likely secure, but in tropical montane catchments, particularly in foreland basins, the contribution of upland, ^{13}C-enriched, plant-

Table 3
Altitude effect demonstrated in dual isotopes for two classes of leaf wax biomarkers.

Site	Elev. (km)	pCO$_2$ (ppmv)	δ^{13}C (‰)				δD (‰)			
			C29alk	se	C28acid	se	C29alk	se	C28acid	se
TAM-06	0.215	389	−39.1	0.7	−35.7	0.6	−168	3	−159	7
TAM-05	0.223	389	−39.3	0.6	−35.5	0.5	−166	3	−153	3
SPD-02	1.494	335	−37.3	0.6	−33.6	0.7	−177	3	−180	5
SPD-01	1.713	327	−36.7	0.7	−34.5	0.9	−176	4	−168	6
ESP-01	2.868	286	−36.0	0.6	−34.0	0.6	−216	3	−212	5
Gradient (‰ km^{-1})			1.28		0.67		−16.5		−19.4	
RMSE			0.36		0.62		10.1		9.9	
Gradient (‰ 100 ppmv^{-1})[a,b]			−3.27		−1.74					
RMSE			0.29		0.58					

We report a summary of data for the homologues of each compound class used in river applications but data for all homologues are found in Appendix A.

[a] Assumes that the dominant control on δ^{13}C$_{wax}$ is pCO$_2$.
[b] The δD value of precipitation is identified as the dominant control of δD$_{wax}$ (Feakins et al., 2016a).

derived contributions should be carefully considered. Findings of an altitude effect in plant wax δ^{13}C are expected to be most pronounced in sedimentary records draining high elevations, when these are a significant proportion of the catchment (Ponton et al., 2014), and when forest productivity, precipitation and erosion rates conspire to make these montane regions a significant source of plant wax to the downstream archive (Hoffmann et al., 2016).

5. CONCLUSIONS

We have conducted a multi-species survey of plant leaf wax carbon isotope biogeochemistry in tropical forests spanning an elevation gradient extending from tropical lowland rainforest to montane cloud forest ecosystems in Perú. Our elevation transect supports the use of leaf wax biomarkers for a range of applications including provenance studies in fluvial transport and paleoaltimetry studies. We find strong evidence for an altitude effect on plant wax δ^{13}C across the profile, mirrored in both biomarker constituents as well as in bulk tissue with offsets well-characterized from large tropical forest sample sets. Notably this change occurs in a context of high species diversity and community turnover in the Andes-Amazon region. While single species transects are not possible, genus and family-specific transects suggest this is a robust response to environment and not solely a function of taxonomic turnover. Our plot-based elevation transect provides new understanding of plant carbon isotopic compositions across tropical lowland rainforest and montane cloud forests. These data can inform future sedimentary applications, including tracking sourcing within the Madre de Dios River network and lowland Amazon basin. More generally, our finding of an altitude effect is consistent with globally compiled data from wet (>1.5 m MAP) climatic regions. The mechanism is likely adiabatic, and our results follow experimental predictions for humid environments that low pCO$_2$ will lead to ^{13}C enrichment of $c.$ +1‰ km^{-1}. Although the altitudinal effect is clear in this humid tropical forest transect, aridity may confound these presumed-adiabatic signals elsewhere. Dual isotope analysis of C and H in plant waxes offers a practical means to monitor for secondary climatic controls.

AUTHOR CONTRIBUTION STATEMENT

M.S.W. led the leaf wax carbon isotope analyses, interpretations and graphed the results. S.J.F designed the leaf wax carbon isotope study and guided interpretations. Y.M., G.P.A., L.P.B., N.S., and A.S., designed the field sampling; L.P.B., N.S., A.S., B.B., conducted CHAMBASA fieldwork. R.E.M. led taxonomy and analyzed bulk leaf carbon isotopic composition. M.S.W., L.P.B., A.S., B.B., analyzed aspects of data. M.S.W contributed and S.J.F. wrote the manuscript.

APPENDIX A. SUPPLEMENTARY MATERIAL

Supplementary data associated with this article can be found, in the online version, at http://dx.doi.org/10.1016/j.gca.2017.02.022. These data include Google maps of the most important areas described in this article.

REFERENCES

Asner G. P., Anderson C. B., Martin R. E., Knapp D. E., Tupayachi R., Sinca F. and Malhi Y. (2014a) Landscape-scale changes in forest structure and functional traits along an Andes-to-Amazon elevation gradient. *Biogeosciences* **11**, 843–856.

Asner G. P., Martin R. E., Tupayachi R., Anderson C. B., Sinca F., Carranza-Jimenéz L. and Martinez P. (2014b) Amazonian functional diversity from forest canopy chemical assembly. *Proc. Natl. Acad. Sci.* **111**, 5604–5609.

Asner G. P., Martin R. E., Anderson C. B., Kryston K., Vaughn N., Knapp D. E., Bentley L. P., Shenkin A., Salinas N., Sinca F., Tupayachi R., Quispe Huaypar K., Montoya Pillco M., Ccori Álvarez F. D., Díaz S., Enquist B. and Malhi Y. (2016) Scale dependence of canopy trait distributions along a tropical forest elevation gradient. *New Phytol.*. http://dx.doi.org/10.1111/nph.14068.

Badewien T., Vogts A. and Rullkotter J. (2015) N-Alkane distribution and carbon stable isotope composition in leaf waxes of C3 and C4 plants from Angola. *Org. Geochem.* **89–90**, 71–79.

Beerling D. J., Lake J. A., Berner R. A., Hickey L. J., Taylor D. W. and Royer D. L. (2002) Carbon isotope evidence implying high O2/CO2 ratios in the Permo-Carboniferous atmosphere. *Geochim. Cosmochim. Acta* **66**, 3757–3767.

Berner R. A., Petsch S. T., Lake J. A., Beerling D. J., Popp B. N., Lane R. S., Laws E. A., Westley M. B., Cassar N., Woodward F. I. and Quick W. P. (2000) Isotope fractionation and atmospheric oxygen: implications for phanerozoic O₂ evolution. *Science* **287**, 1630–1633.

Bi X., Sheng G., Liu X., Li C. and Fu J. (2005) Molecular and carbon and hydrogen isotopic composition of *n*-alkanes in plant leaf waxes. *Org. Geochem.* **36**, 1405–1417.

Brüggemann N., Gessler A., Kayler Z., Keel S. G., Badeck F., Barthel M., Boeckx P., Buchmann N., Brugnoli E., Esperschütz

J., Gavrichkova O., Ghashghaie J., Gomez-Casanovas N., Keitel C., Knohl A., Kuptz D., Palacio S., Salmon Y., Uchida Y. and Bahn M. (2011) Carbon allocation and carbon isotope fluxes in the plant-soil-atmosphere continuum: a review. *Biogeosciences* **8**, 3457–3489.

Castaneda I. S., Mulitza S., Schefuß E., Lopes dos Santos R. A., Sinninghe Damste J. S. and Schouten S. (2009) Wet phases in the Sahara/Sahel region and human migration patterns in North Africa. *Proc. Natl. Acad. Sci.* **106**, 20159–20163.

Cerling T. E., Wynn J. G., Andanje S. A., Bird M. I., Korir D. K., Levin N. E., Mace W., Macharia A. N., Quade J. and Remien C. H. (2011) Woody cover and hominin environments in the past 6 million years. *Nature* **476**, 51–56.

Cernusak L. A., Ubierna N., Winter K., Holtum J. A. M., Marshall J. D. and Farquhar G. D. (2013) Environmental and physiological determinants of carbon isotope discrimination in terrestrial plants. *New Phytol.* **200**, 950–965.

Chikaraishi Y. and Naraoka H. (2003) Compound-specific δ^{13}C–δD analyses of *n*-alkanes extracted from terrestrial and aquatic plants. *Phytochemistry* **63**, 361–371.

Chikaraishi Y., Naraoka H. and Poulson S. R. (2004) Carbon and hydrogen isotopic fractionation during lipid biosynthesis in a higher plant (Cryptomeria japonica). *Phytochemistry* **65**, 323–330.

Chikaraishi Y. and Naraoka H. (2007) Δ^{13}C and δD relationships among three n-alkyl compound classes (*n*-alkanoic acid, *n*-alkane and n-alkanol) of terrestrial higher plants. *Org. Geochem.* **38**, 198–215.

Cohen E. R., Cvitaš T., Frey J. G., Holmström B., Kuchitsu K., Marquardt R., I Mills F. P., Quack M., Stohner J., Strauss H. L., Takami M. and Thor A. J. (2007) *Quantities, Units and Symbols in Physical Chemistry*, third ed. Royal Society of Chemistry Publishing, Cambridge, UK, p. 265.

Collister J. W., Rieley G., Stern B., Eglinton G. and Fry B. (1994) Compound-specific δ^{13}C analyses of leaf lipids from plants with differing carbon dioxide metabolisms. *Org. Geochem.* **21**, 619–627.

Conte M. H., Weber J. C., Carlson P. J. and Flanagan L. B. (2003) Molecular and carbon isotopic composition of leaf wax in vegetation and aerosols in a northern prairie ecosystem. *Oecologia* **135**, 67–77.

Diefendorf A. F., Mueller K. E., Wing S. L., Koch P. L. and Freeman K. H. (2010) Global patterns in leaf ^{13}C discrimination and implications for studies of past and future climate. *Proc. Natl. Acad. Sci.* **107**, 5738–5743.

Diefendorf A. F., Freeman K. H., Wing S. L., Currano E. D. and Mueller K. E. (2015) Paleogene plants fractionated carbon isotopes similar to modern plants. *Earth Planet. Sci. Lett.* **429**, 33–44.

Diefendorf A. F. and Freimuth E. J. (2017) Extracting the most from terrestrial plant-derived n-alkyl lipids and their carbon isotopes from the sedimentary record: A review. *Org. Geochem.* **103**, 1–21.

Eglinton G. and Hamilton R. (1967) Leaf epicuticular waxes. *Science* **156**, 1322–1335.

Ernst N., Peterse F., Breitenbach S. F. M., Syiemlieh H. J. and Eglinton T. I. (2013) Biomarkers record environmental changes along an altitudinal transect in the wettest place on Earth. *Org. Geochem.* **60**, 93–99.

Farquhar G. D., Ehleringer J. R. and Hubick K. T. (1989) Carbon isotope discrimination and photosynthesis. *Ann. Rev. Plant Physiol. Plant Mol. Biol.* **40**, 503–537.

Feakins S., deMenocal P. and Eglinton T. (2005) Biomarker records of Late Neogene Changes in East African Vegetation. *Geology* **33**, 977–980.

Feakins S., Levin N., Liddy H., Sieracki A., Eglinton T. and Bonnefille R. (2013) Northeast African vegetation change over 12 million years. *Geology* **41**, 295–298.

Feakins S. J., Bentley L. P., Salinas N., Shenkin A., Blonder B., Goldsmith G. R., Ponton C., Arvin L. J., Wu M. S., Peters T., West A. J., Martin R. E., Enquist B. J., Asner G. P. and Malhi Y. (2016a) Plant leaf wax biomarkers capture gradients in hydrogen isotopes of precipitation from the Andes and Amazon. *Geochim. Cosmochim. Acta* **182**, 155–172.

Feakins S. J., Peters T., Wu M. S., Shenkin A., Salinas N., Girardin C. A. J., Bentley L. P., Blonder B., Enquist B. J., Martin R. E., Asner G. P. and Malhi Y. (2016b) Production of leaf wax *n*-alkanes across a tropical forest elevation transect. *Org. Geochem.* **100**, 89–100.

Freeman K. H. and Colarusso L. A. (2001) Molecular and isotopic records of C4 grassland expansion in the late Miocene. *Geochim. Cosmochim. Acta* **65**, 1439–1454.

Freeman K. H. and Pancost R. D. (2014) *Biomarkers for Terrestrial Plants and Climate, Treatise on Geochemistry, second ed.*. JAI-Elsevier Science Inc, pp. 395–416.

Friend A. D., Woodward F. I. and Switsur V. R. (1989) Field measurements of photosynthesis, stomatal conductance, leaf nitrogen and $\delta^{13}C$ along altitudinal gradients in Scotland. *Funct. Ecol.* **3**, 117–122.

Galy V., Eglinton T., France-Lanord C. and Sylva S. (2011) The provenance of vegetation and environmental signatures encoded in vascular plant biomarkers carried by the Ganges-Brahmaputra rivers. *Earth Planet. Sci. Lett.* **304**, 1–12.

Garcin Y., Schefuß E., Schwab V. F., Garreta V., Gleixner G., Vincens A., Todou G., Séné O., Onana J.-M., Achoundong G. and Sachse D. (2014) Reconstructing C3 and C4 vegetation cover using n-alkane carbon isotope ratios in recent lake sediments from Cameroon, Western Central Africa. *Geochim. Cosmochim. Acta* **142**, 482–500.

Ghosh P. and Brand W. A. (2003) Stable isotope ratio mass spectrometry in global climate change research. *Int. J. Mass Spectrom.* **228**, 1–33.

Girardin C. A. J., Farfan-Rios W., Garcia K., Feeley K. J., Jorgensen P. M., Murakami A. A., Perez L. C., Seidel R., Paniagua N., Claros A. F. F., Maldonado C., Silman M., Salinas N., Reynel C., Neill D. A., Serrano M., Caballero C. J., Cuadros M. D. L., Macia M. J., Killeen T. J. and Malhi Y. (2014) Spatial patterns of above-ground structure, biomass and composition in a network of six Andean elevation transects. *Plant Ecol. Divers.* **7**, 161–171.

Goldsmith G. R., Bentley L. P., Shenkin A., Salinas N., Blonder B., Martin R. E., Castro-Ccossco R., Chambi-Porroa P., Diaz S., Enquist B. J., Asner G. P. and Malhi Y. (2016) Variation in leaf wettability traits along a tropical montane elevation gradient. *New Phytol.*. http://dx.doi.org/10.1111/nph.14121.

Graham H. V., Patzkowsky M. E., Wing S. L., Parker G. G., Fogel M. L. and Freeman K. H. (2014) Isotopic characteristics of canopies in simulated leaf assemblages. *Geochim. Cosmochim. Acta* **144**, 82–95.

Häggi C., Sawakuchi A. O., Chiessi C. M., Mulitza S., Mollenhauer G., Sawakuchi H. O., Baker P. A., Zabel M. and Schefuß E. (2016) Origin, transport and deposition of leaf-wax biomarkers in the Amazon Basin and the adjacent Atlantic. *Geochim. Cosmochim. Acta* **192**, 149–165.

Hayes J. (1993) Factors controlling the ^{13}C content of sedimentary organic compounds: principals and evidence. *Mar. Geol.* **113**, 111–125.

Hemingway J. D., Schefuß E., Dinga B. J., Pryer H. and Galy V. V. (2016) Multiple plant-wax compounds record differential sources and ecosystem structure in large river catchments. *Geochim. Cosmochim. Acta* **184**, 20–40.

Hoch G. and Körner C. (2012) Global patterns of mobile carbon stores in trees at the high-elevation tree line. *Glob. Ecol. Biogeogr.* **21**, 861–871.

Hoffmann B., Feakins S. J., Bookhagen B., Olen S. M., Adhikari D. P., Mainali J. and Sachse D. (2016) Climatic and geomorphic drivers of plant organic matter transport in the Arun River, E Nepal. *Earth Planet. Sci. Lett.* **452**, 104–114.

Hren M. T., Pagani M., Erwin D. M. and Brandon M. (2010) Biomarker reconstruction of the early Eocene paleotopography and paleoclimate of the northern Sierra Nevada. *Geology* **38**, 7–10.

Huang Y., Street-Perrott F. A., Metcalfe S. E., Brenner M., Moreland M. and Freeman K. H. (2001) Climate change as the dominant control on glacial-interglacial variations in C3 and C4 plant abundance. *Science* **293**, 1647–1651.

Huntington K. W., Wernicke B. P. and Eiler J. M. (2010) Influence of climate change and uplift on Colorado Plateau paleotemperatures from carbonate clumped isotope thermometry. *Tectonics* **29**, TC3005.

Kar N., Garzione C. N., Jaramillo C., Shanahan T., Carlotto V., Pullen A., Moreno F., Anderson V., Moreno E. and Eiler J. (2016) Rapid regional surface uplift of the northern Altiplano plateau revealed by multiproxy paleoclimate reconstruction. *Earth Planet. Sci. Lett.* **447**, 33–47.

Keeling C. D., Piper S. C., Bacastow R. B., Wahlen M., Whorf T. P., Heimann M. and Meijer H. A. (2001) *Exchanges of atmospheric CO2 and 13CO2 with the terrestrial biosphere and oceans from 1978 to 2000. I. Global aspects, SIO Reference Series.*. Scripps Institution of Oceanography, San Diego, p. 88.

Kenzo T., Inoue Y., Yoshimura M., Yamashita M., Tanaka-Oda A. and Ichie T. (2015) Height-related changes in leaf photosynthetic traits in diverse Bornean tropical rain forest trees. *Oecologia* **177**, 191–202.

Kohn M. (2016) Carbon isotope discrimination in C3 land plants is independent of natural variations in pCO_2. *Geochem. Perspectives Lett.* **2**, 35–43.

Körner C., Farquhar G. D. and Roksandic Z. (1988) A global survey of carbon isotope discrimination in plants from high altitude. *Oecologia* **74**, 623–632.

Körner C., Farquhar G. D. and Wong S. C. (1991) Carbon isotope discrimination by plants follows latitudinal and altitudinal trends. *Oecologia* **88**, 30–40.

Körner C. (2007) The use of 'altitude' in ecological research. *Trends Ecol. Evol.* **22**, 569–574.

Kreft H. and Jetz W. (2007) Global patterns and determinants of vascular plant diversity. *Proc. Natl. Acad. Sci.* **104**, 5925–5930.

Magill C. R., Ashley G. M. and Freeman K. H. (2013) Ecosystem variability and early human habitats in eastern Africa. *Proc. Natl. Acad. Sci.* **110**, 1167–1174.

Malhi Y., Girardin C. and Goldsmith G. R., et al. (2016) The variation of productivity and its allocation along a tropical elevation gradient: a whole carbon budget perspective. *New Phytol.*. http://dx.doi.org/10.1111/nph.14189.

Marthews T., Riutta T., Oliveras Menor I., Urrutia R., Moore S., Metcalfe D., Malhi Y., Phillips O., Huaraca Huasco W., Ruiz Jaén M., Girardin C., Butt N. and Cain R. (2014) Measuring tropical forest carbon allocation and cycling: a RAINFOR-GEM field manual for intensive census plots (v3.0). *Manual, Global Ecosyst. Monit. Network*. http://dx.doi.org/10.5287/bodleian:xp68kh42k.

McDowell N. G., Bond B. J., Dickman L. T., Ryan M. G. and Whitehead D. (2011) Relationships between tree height and carbon isotope discrimination. In *Size- and Age-Related Changes in Tree Structure and Function* (eds. C. F. Meinzer, B. Lachenbruch and E. T. Dawson). Springer, Netherlands, Dordrecht, pp. 255–286.

Olsen S. C. and Randerson J. T. (2004) Differences between surface and column atmospheric CO_2 and implications for carbon cycle research. *J. Geophys. Res.: Atmos.* **109**, D02301.

Poage M. A. and Chamberlain C. P. (2001) Empirical relationships between elevation and the stable isotope composition of precipitation and surface waters: Considerations for studies of paleoelevation change. *Am. J. Sci.* **301**, 1–15.

Polissar P. J., Freeman K. H., Rowley D. B., McInerney F. A. and Currie B. S. (2009) Paleoaltimetry of the Tibetan Plateau from D/H ratios of lipid biomarkers. *Earth Planet. Sci. Lett.* **287**, 64–76.

Ponton C., West A. J., Feakins S. J. and Galy V. (2014) Leaf wax biomarkers in transit record river catchment composition. *Geophys. Res. Lett.* **41**, 6420–6427.

Quade J., Breecker D. O., Daeron M. and Eiler J. (2011) The paleoaltimetry of Tibet: an isotopic perspective. *Am. J. Sci.* **311**, 77–115.

Quade J., Eiler J., Daeron M. and Achyuthan H. (2013) The clumped isotope geothermometer in soil and paleosol carbonate. *Geochim. Cosmochim. Acta* **105**, 92–107.

Schefuß E., Schouten S., Jansen J. H. F. and Damste J. S. S. (2003) African vegetation controlled by tropical sea surface temperatures in the mid-Pleistocene period. *Nature* **422**, 418–421.

Schubert B. A. and Jahren A. H. (2012) The effect of atmospheric CO_2 concentration on carbon isotope fractionation in C_3 land plants. *Geochim. Cosmochim. Acta* **96**, 29–43.

Tao S. Q., Eglinton T. I., Montlucon D. B., McIntyre C. and Zhao M. X. (2015) Pre-aged soil organic carbon as a major component of the Yellow River suspended load: Regional significance and global relevance. *Earth Planet. Sci. Lett.* **414**, 77–86.

Ter Steege H.ATDN (Amazon Tree Diversity Network: collective author)RAINFOR (The Amazon Forest Inventory Network: collective author) (2010) Contribution of current and historical processes to patterns of tree diversity and composition of the Amazon. In *Amazonia: Landscape and Species Evolution* (eds. C. Hoorn and F. P. Wesselingh). Wiley, Oxford, pp. 349–359.

Terashima I., Masuzawa T., Ohba H. and Yokoi Y. (1995) Is photosynthesis suppressed at higher elevations due to low CO_2 pressure? *Ecology* **76**, 2663–2668.

Tipple B. J., Pagani M., Krishnan S., Dirghangi S. S., Galeotti S., Agnini C., Giusberti L. and Rio D. (2011) Coupled high-resolution marine and terrestrial records of carbon and hydrologic cycles variations during the Paleocene-Eocene Thermal Maximum (PETM). *Earth Planet. Sci. Lett.* **311**, 82–92.

Vitousek P. M., Field C. B. and Matson P. A. (1990) Variation in foliar $\delta^{13}C$ in Hawaiian Metrosideros polymorpha: a case of internal resistance? *Oecologia* **84**, 362–370.

Vogts A., Moossen H., Rommerskirchen F. and Rullkotter J. (2009) Distribution patterns and stable carbon isotopic composition of alkanes and alkan-1-ols from plant waxes of African rain forest and savanna C3 species. *Org. Geochem.* **40**, 1037–1054.

Wei K. and Jia G. (2009) Soil n-alkane $\delta^{13}C$ along a mountain slope as an integrator of altitude effect on plant species $\delta^{13}C$. *Geophys. Res. Lett.* **36**, L11401.

Whiteside J. H., Olsen P. E., Eglinton T., Brookfield M. E. and Sambrotto R. N. (2010) Compound-specific carbon isotopes from Earth's largest flood basalt eruptions directly linked to the end-Triassic mass extinction. *Proc. Natl. Acad. Sci.* **107**, 6721–6725.

Zhou Y. P., Grice K., Stuart-Williams H., Farquhar G. D., Hocart C. H., Lu H. and Liu W. G. (2010) Biosynthetic origin of the saw-toothed profile in $\delta^{13}C$ and δ^2H of n-alkanes and systematic isotopic differences between n-, iso- and anteiso-alkanes in leaf waxes of land plants. *Phytochemistry* **71**, 388–403.

Zhou Y., Stuart-Williams H., Grice K., Kayler Z. E., Zavadlav S., Vogts A., Rommerskirchen F., Farquhar G. D. and Gessler A. (2015) Allocate carbon for a reason: Priorities are reflected in the $^{13}C/^{12}C$ ratios of plant lipids synthesized via three independent biosynthetic pathways. *Phytochemistry* **111**, 14–20.

Zhu Y., Siegwolf R. T. W., Durka W. and Körner C. (2010) Phylogenetically balanced evidence for structural and carbon isotope responses in plants along elevational gradients. *Oecologia* **162**, 853–863.

Associate editor: Ann Pearson